This article has been accepted for publication in IEEE Communications Letters. This is the author's version which has not been fully edited and content may change prior to final publication. Citation information: DOI 10.1109/LCOMM.2023.3325662

Stochastic Coverage Analysis for Multi-Altitude LEO Satellite Networks

Niloofar Okati and Taneli Riihonen, *Senior Member, IEEE*

***Abstract*—While leading companies will soon have launched their low Earth orbit (LEO) constellations with different orbital characteristics, e.g., altitude and inclination, the analytical understanding of these networks with satellites flying on varying altitudes is only limited to specific network setups, e.g., polar orbits. In this letter, we derive the coverage probability of a generic multi-altitude LEO network with the satellites being distributed uniformly on inclined circular orbits at varying altitudes. To maintain tractability of our derivations, we firstly model the satellites as a binomial point process assuming their altitude to be an arbitrarily distributed random variable. Secondly, we take into account the latitude-dependent distribution of satellites over the orbits through finding the effective number of satellites. The coverage probabilities of four multi-altitude benchmark constellations are evaluated in terms of different constellation parameters as well as the user's latitude. The numerical results reveal that after a certain limit, the coverage probability improves only slightly with increasing the constellation size; therefore, the costly over-sizing of LEO networks is not always recommendable.**

***Index Terms*—Communication satellite networks, low Earth orbit (LEO), coverage probability, stochastic geometry.**

I. Introduction

THE great potential of low Earth orbit (LEO) communication satellites for providing global broadband connectivity—especially for remote regions or countries with restricted Internet access—is encouraging many companies to launch their Internet constellations to 500–2000 km altitudes. To keep pace with the rapid commercial progress of LEO networks, the scientific understanding of their performance in terms of the network parameters is crucial for the future developments.

In this letter, we analyze the coverage probability of a massive multi-altitude LEO constellation in which the satellites fly on different altitudes. The general multi-altitude setup corresponds to several scenarios: (i) deploying the satellites of a constellation at different shells, e.g., Starlink; (ii) elliptical orbits for which the altitude varies with true anomaly of a satellite; and (iii) the inter-operation of several constellations at different altitudes to maximize resource sharing opportunities.

The application of stochastic geometry for tractable analysis of large-scale massive wireless networks [1] has been recently extended to LEO satellite systems. The mobility of satellites over the orbits results in different realizations of satellites' locations over time which can be modeled by a spatial point process to facilitate the utilization of the tools from stochastic geometry [2]–[4]. A stochastic geometry-based framework is provided in [2] for modeling and performance analysis of a single-altitude LEO constellation by modeling the network as a binomial point process (BPP) that captures the locality characteristics of a limited number of nodes distributed in a finite region. The inherent mismatch between the performance of a BPP distributed constellation and an actual constellation, caused by an uneven distribution of satellites along different latitudes, is compensated numerically in [2] and analytically adjusted in [3] through finding a latitude-dependent parameter. In [4], the non-uniform distribution of satellites is modeled as a nonhomogeneous Poisson point process (PPP), with its intensity being the actual latitude-dependent distribution of satellites on an orbital shell.

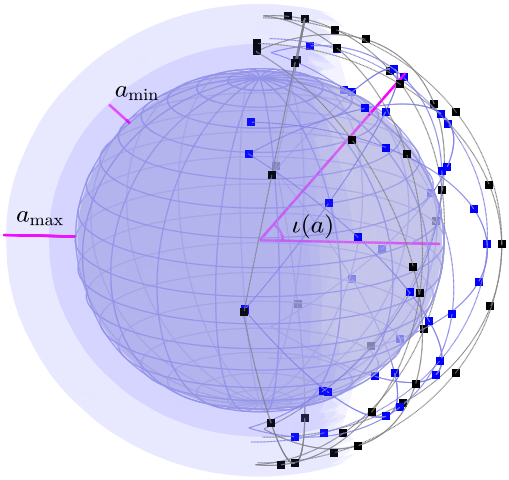

Fig. 1. A multi-altitude network consisting of several constellations deployed at different altitudes ranging from $a_{\min}$ to $a_{\max}$.

Only [5], being the most relevant reference for our study, formulate the distance distributions and coverage probability for a LEO network when satellites are distributed on multiple concentric spheres with specific known radii. Comparing with [5], this letter adds the following advantages: (i) the analysis is applicable to more generic highly massive networks with any number of altitudinal levels without affecting its complexity; (ii) it includes the inclination angle of satellites in the analysis; and (iii) it takes into account the nonuniform density of satellites along different latitudes.

To tractably analyze the coverage performance of a multi-altitude LEO network, we model the satellites as a BPP on an orbital shell with an arbitrarily distributed radius. The mismatch between the performance of the BPP distributed constellation and the actual constellation is compensated by derivation of the so-called effective number of satellites. The analytical derivations are verified through Monte Carlo simulations while showing the effects of different parameters, e.g., the constellation size and the user's latitude on the coverage performance for several multi-altitude constellations.

Niloofar Okati is with Nokia Bell Labs, Karaportti 3, FI-02610 Espoo, Finland (niloofar.okati@nokia-bell-labs.com). Taneli Riihonen is with Unit of Electrical Engineering, Faculty of Information Technology and Communication Sciences, Tampere University, FI-33720 Tampere, Finland (taneli.riihonen@tuni.fi). The work was supported by a Nokia University Donation.

II. System Model

A LEO multi-altitude constellation is adopted as the system model in this paper, shown in Fig. 1. The constellation consists of $N_{\rm act}$ satellites distributed uniformly on circular orbits with different altitudes, ranging from $a_{\min}$ to $a_{\max}$. The orbits can be inclined at different angles denoted by $\iota(a)$ which is a function of network's parameters, viz. altitude a.

The user is located at a specific latitude, denoted by $\phi_{\rm u}$, on Earth's surface that is assumed to be a perfect sphere with radius $r_\oplus \approx 6371$ km. The user may be connected only to those satellites which are elevated above the user's horizon at least to an angle of $\theta_{\min}$. Correspondingly, the maximum possible distance at which a user is able to communicate with a satellite, denoted by $r_{\max}(a)$, is obtained as a function of altitude as $\frac{r_{\max}(a)}{r_\oplus} = \sqrt{\frac{a}{r_\oplus}\left(\frac{a}{r_\oplus}+2\right)+\sin^2(\theta_{\min})}-\sin(\theta_{\min})$.

We refer to a serving satellite as the nearest satellite to the user. All other visible satellites may cause co-channel interference due to implementing frequency reuse by assuming K orthogonal frequency channels, with $K \leq N_{\rm act}$, and randomly assigning a subset of $N_{\rm act}/K$ satellites to each channel. The ground user is associated with the frequency channel that is assigned to the serving satellite. The distance from the user to any satellite is denoted by R_n, $n = 0, 1, 2, \ldots, N_{\rm act}-1$, while their corresponding channel gains are H_n, $n = 0, 1, 2, \ldots, N_{\rm act}-1$. The subscript zero associates the parameter with the serving satellite. Due to Earth's blockage, it is obvious that $H_n = 0$ for $R_n > r_{\max}$.

The satellites have directional antennas with their beams radiating towards the ground users. The ground terminal is equipped with a phased array antenna which is capable of tracking the serving satellite to maintain a connection. The reception of the signal may be subject to interference due to lack of full alignment between the terminals' and satellites' beams and/or existence of side lobes in their radiation patterns. We also assume that satellites' antenna gains and their altitude are proportional for compensating for the more severe path loss of higher altitudes. Thus, the satellites' and the user's antenna gains are denoted by $G_n(a)$ and $G_{\rm u}$, respectively.

Consequently, the signal-to-interference-plus-noise ratio (SINR) for any arbitrary user on Earth is given by

$$\mathrm{SINR} \triangleq \frac{p_{\rm t} G_{\rm t}(a) H_0 R_0^{-\alpha}}{I+\sigma^2}, \tag{1}$$

where $p_{\rm t}$ is the transmit power, α is a path-loss exponent, $G_{\rm t}(a) = G_{\rm u} G_n(a)$ is the overall antenna gain, σ^2 is the additive noise power, and $I \triangleq \sum_{n=1}^{N_{\rm I}} p_{\rm t} G_{\rm t}(a) H_n R_n^{-\alpha}$ is the cumulative interference power from $N_{\rm I} \leq N_{\rm act}/K - 1$ satellites above the user's horizon that share the same frequency channel with the serving satellite.

III. Stochastic Coverage Analysis

To contribute an analytical expression for coverage performance, we abstract and remodel the above-mentioned physical model as follows. We assume that satellites are distributed according to a BPP on a sphere with radius $A + r_\oplus$, where A is a random altitude ranging from $a_{\min}$ to $a_{\max}$. Using this model, we are able to find the distribution of the serving distance in terms of the cumulative density function (CDF) and the probability density function (PDF). We refer to the total number of satellites in the modeled network as the effective number of satellites, denoted by $N_{\rm eff}$, which enables us to correct the performance mismatch between the theoretical BPP constellation and the actual physical constellation caused by the varying density of satellites over different latitudes: $N_{\rm eff}$ is a function of the actual number of satellites, $N_{\rm act}$, and is derived in the following proposition as a generalization of the results given in [3] from single- to multi-altitude networks.

Proposition 1. *The effective number of satellites for a given user's latitude, which is the total number of satellites presumed by the user from its perspective when expecting the same density continues everywhere, is* $N_{\rm eff} \triangleq 2\, f_{\Phi_{\rm s}}(\phi_{\rm s}) \int_{a_{\min}}^{a_{\max}} N_{\rm s}(a) f_A(a) da / \cos(\phi_{\rm s})$*, where* $\Phi_{\rm s}$ *is a random variable denoting a satellite's latitude with* $f_{\Phi_{\rm s}}(\phi_{\rm s})$ *being the corresponding PDF and* $N_{\rm s}(a)$ *represents the actual number of satellites on an orbital shell at altitude* a*.*

Proof. Assuming that there are $N_{\rm eff}$ uniformly distributed satellites in the sky between the two orbital shells at altitudes $a_{\min}$ and $a_{\max}$, the effective density is given by $\delta_{\rm eff} = \frac{N_{\rm eff}}{v}$ where $v = \frac{4}{3}\pi\left(\left(a_{\max}+r_\oplus\right)^3 - \left(a_{\min}+r_\oplus\right)^3\right)$ is the volume between the two spherical shells. The actual density of satellites in the volume element at latitude $\phi_{\rm s}$ is

$$\delta_{\rm act} = \frac{\left(\int_{a_{\min}}^{a_{\max}} N_{\rm s}(a) f_{\Phi_{\rm s},A}(\phi_{\rm s}, a) da\right) d\phi_{\rm s}}{\frac{v}{2}\cos(\phi_{\rm s})\, d\phi_{\rm s}}. \tag{2}$$

The volume of the spherical shell elements, bounded by $a_{\min}+r_\oplus$ and $a_{\max}+r_\oplus$, and the number of satellites inside the element are given in the denominator and nominator of (2), respectively. As $\Phi_{\rm s}$ and A are assumed to be independent random variables, we have $f_{\Phi_{\rm s},A}(\phi_{\rm s}, a) = f_{\Phi_{\rm s}}(\phi_{\rm s}) f_A(a)$, resulting in $\int_{a_{\min}}^{a_{\max}} f_{\Phi_{\rm s},A}(\phi_{\rm s}, a) da = f_{\Phi_{\rm s}}(\phi_{\rm s}) \int_{a_{\min}}^{a_{\max}} N_{\rm s}(a) f_A(a) da$. The proof is concluded by setting $\delta_{\rm eff} = \delta_{\rm act}$. □

Lemma 1. *In a multi-altitude network, when satellites of each constellation are distributed uniformly on low Earth orbits, the PDF of satellites' latitude,* $\phi_{\rm s}$*, is*

$$f_{\Phi_{\rm s}}(\phi_{\rm s}) = \int_{a_{\min}}^{a_{\max}} \frac{\sqrt{2}}{\pi} \cdot \frac{\cos(\phi_{\rm s})}{\sqrt{\cos(2\phi_{\rm s}) - \cos(2\iota(a))}} f_A(a)\, da, \tag{3}$$

where $f_A(a)$ *is the PDF of the altitude.*

Proof. The distribution of satellites' latitude for a constellation with fixed altitude and the inclination angle is given in [3, Lemma 2]. Generalizing the inclination angle in the multi-altitude network to be altitude-dependent and taking the expectation with respect to A completes the proof. □

In the following lemmas, we will obtain the CDF and PDF of the relative distances between the user and the satellites.

Lemma 2. *The CDF of the distance* R *from the user to any satellite in the multi-altitude network is*

$$F_R(r) \triangleq \mathbb{P}(R \leq r) = \int_l^u \frac{r^2 - a^2}{4 r_\oplus (r_\oplus + a)} f_A(a)\, da + F_A(\min(a_{\max}, r - 2r_\oplus)) - F_A(a_{\min}), \tag{4}$$

where $l=\max(a_{\min}, r-2r_{\oplus})$, $u=\min(a_{\max}, r)$, *and* $f_A(a)$ *and* $F_A(a)$ *are the PDF and the CDF of the altitude, respectively. Using the Leibniz rule, the corresponding PDF is*

$$f_R(r)=\int_l^u \frac{r f_A(a)}{2r_{\oplus}(r_{\oplus}+a)}\,da + f_A(r-2r_{\oplus})H(a_{\max}-r+2r_{\oplus}) \tag{5}$$
$$+\frac{f_A(u)\big(r^2-u^2\big)H(a_{\max}-r)}{4r_{\oplus}(r_{\oplus}+u)} - \frac{f_A(l)\big(r^2-l^2\big)H(r-2r_{\oplus}-a_{\min})}{4r_{\oplus}(r_{\oplus}+l)},$$

where $H(\cdot)$ *is the Heaviside step function.*

Proof. Using the law of total probability, we have $\mathbb{P}(R\le r)=\mathbb{E}_A\left[\mathbb{P}(R\le r|A=a)\right]$ where $\mathbb{P}(R\le r|A=a)$ is the CDF of R for a single-altitude network given in [2, Lemma. 1]. □

Noting that $f_A(a)=\frac{1}{a_{\max}-a_{\min}}$ for uniformly distributed A results in the following distribution for R in the special case.

Corollary 1. *When* A *is a uniform random variable, i.e.,* $A\sim\mathcal{U}(a_{\min}, a_{\max})$*, the PDF of* R *can be written as*

$$f_R(r)=\begin{cases}\frac{r\ln\left(\frac{r_{\oplus}+a_{\max}}{r_{\oplus}+a_{\min}}\right)}{2r_{\oplus}(a_{\max}-a_{\min})}, & r-2r_{\oplus}\le a_{\min}\le a_{\max}\le r,\\ \frac{r\ln\left(\frac{r_{\oplus}+r}{r_{\oplus}+a_{\min}}\right)}{2r_{\oplus}(a_{\max}-a_{\min})}, & r-2r_{\oplus}<a_{\min}<r<a_{\max},\\ \frac{r\ln\left(\frac{r_{\oplus}+a_{\max}}{r-r_{\oplus}}\right)-2r_{\oplus}}{2r_{\oplus}(a_{\max}-a_{\min})}+\frac{1}{a_{\max}-a_{\min}}, & a_{\min}<r-2r_{\oplus}<a_{\max}<r,\\ 0, & \textit{otherwise}.\end{cases} \tag{6}$$

For a single-altitude constellation, i.e., $a_{\max}=a_{\min}=a$, the PDF of R can be obtained from (6) as $f_R(r)=\frac{r}{2r_{\oplus}(r_{\oplus}+a)}$ for $a\le r\le 2r_{\oplus}+a$ while $f_R(r)=0$ otherwise. As expected, the expression is similar to our derivation in [2, Lemma 1]. The distribution of the serving distance is given as follows using the distribution of R given in Lemma 2 and Corollary 1. The PDF of the serving distance R_0 is given in [2, Lemma 2] by $f_{R_0}(r_0)=N_{\text{eff}}\left(1-F_R(r_0)\right)^{N_{\text{eff}}-1}f_R(r_0)$ for $a_{\min}\le r_0\le 2r_{\oplus}+a_{\max}$ while $f_{R_0}(r_0)=0$ otherwise.

The above distance distributions will be used to derive coverage probability in the multi-altitude network. Let us begin with the definition of the coverage probability which is the probability that the SINR at the user's receiver is greater than some minimum required SINR, denoted by T:

$$P_{\text{c}}(T)\triangleq\mathbb{P}(\text{SINR}>T)=\mathbb{P}\left(\frac{p_{\text{t}}G_{\text{t}}(A)H_0R_0^{-\alpha}}{I+\sigma^2}>T\right). \tag{7}$$

In the following proposition whose accuracy is verified in Fig. 2, we derive an analytical expression for the probability of coverage based on the above definition.

Proposition 2. *The probability of coverage for a user on Earth's surface under a Nakagami fading serving channel when both shape and rate parameters of gamma distribution (square of Nakagami random variables) are set to* m_0*, is*

$$P_{\text{c}}=P_0\,\mathbb{P}(\text{SNR}>T)+(1-P_0)\,\mathbb{P}(\text{SINR}>T|I>0), \tag{8}$$

where $P_0=\left(1-\frac{2r_{\oplus}A-r_0^2+A^2}{4r_{\oplus}(r_{\oplus}+A)-r_0^2+A^2}\right)^{\frac{N_{\text{eff}}}{K}-1}$ *is the probability of having no visible interfering satellite [2],*

$$\mathbb{P}(\text{SNR}>T)=\int_{a_{\min}}^{a_{\max}}\int_{a_{\min}}^{r_{\max}} f_A(a)f_{R_0}(r_0)e^{-s\sigma^2}\sum_{k=0}^{m_0-1}\frac{\left(s\sigma^2\right)^k}{k!}\,dr_0da, \tag{9}$$

TABLE I
FOUR MULTI-ALTITUDE BENCHMARK CONSTELLATIONS

Constellations	I Starlink	II Starlink	III Kuiper	IV Telesat
No. orbital shells	3	4	3	3
Discrete altitudes	335 km	540 km	590 km	1000 km
	340 km	550 km	610 km	1200 km
	345 km	560 km	630 km	1325 km
	—	570 km	—	—
Inclination angles	42°	53°	33°	98.8°
	48°	53°	42°	87°
	53°	97.6°	52°	51°
	—	70°	—	—
Main lobe gains	12 dBi	16 dBi	17 dBi	22 dBi

with $s=\frac{m_0Tr_0^{\alpha}}{p_{\text{t}}G_{\text{t}}(a)}$*, and*

$$\mathbb{P}(\text{SINR}>T|I>0)=\int_{a_{\min}}^{a_{\max}}\int_{a_{\min}}^{r_{\max}} f_A(a)f_{R_0}(r_0)\,e^{-s\sigma^2} \cdot\sum_{k=0}^{m_0-1}\frac{\sum_{l=0}^{k}\binom{k}{l}\left(s\sigma^2\right)^l(-s)^{k-l}\frac{\partial^{k-l}}{\partial s^{k-l}}\mathcal{L}_I(s)}{k!}\,dr_0da, \tag{10}$$

where $\mathcal{L}_I(s)$ *is the Laplace function of interference power,* I*.*

Proof. Using the definition of coverage probability, we obtain the proof by deriving the expression for the case of having non-zero interference, i.e., the second term in 8, as

$$\begin{aligned}
&\mathbb{E}_{R_0,A}\left[(1-P_0)\mathbb{P}(\text{SINR}>T|R_0=r_0,A=a)\right]\\
&=\int_{a_{\min}}^{a_{\max}}\int_{a_{\min}}^{r_{\max}}(1-P_0)f_A(a)f_{R_0}(r_0)\\
&\qquad\cdot\mathbb{P}\left(H_0>\frac{Tr_0^{\alpha}\left(I+\sigma^2\right)}{p_{\text{t}}G_{\text{t}}(a)}\right)\,dr_0da,\\
&\overset{(a)}{=}\int_{a_{\min}}^{a_{\max}}\int_{a_{\min}}^{r_{\max}}(1-P_0)f_A(a)f_{R_0}(r_0)\\
&\qquad\cdot\mathbb{E}_I\left[\frac{\Gamma\left(m_0,m_0\frac{Tr_0^{\alpha}\left(I+\sigma^2\right)}{p_{\text{t}}G_{\text{t}}(a)}\right)}{\Gamma(m_0)}|I>0\right]dr_0da,\\
&\overset{(b)}{=}\int_{a_{\min}}^{a_{\max}}\int_{a_{\min}}^{r_{\max}}(1-P_0)f_A(a)f_{R_0}(r_0)\,e^{-\frac{m_0Tr_0^{\alpha}\sigma^2}{p_{\text{t}}G_{\text{t}}(a)}}\mathbb{E}_I\Bigg[e^{-\frac{m_0Tr_0^{\alpha}I}{p_{\text{t}}G_{\text{t}}(a)}}\\
&\cdot\sum_{k=0}^{m_0-1}\frac{\sum_{l=0}^{k}\binom{k}{l}\left(\frac{m_0Tr_0^{\alpha}\sigma^2}{p_{\text{t}}G_{\text{t}}(a)}\right)^l\left(\frac{m_0Tr_0^{\alpha}I}{p_{\text{t}}G_{\text{t}}(a)}\right)^{k-l}}{k!}\Bigg]dr_0da,
\end{aligned} \tag{11}$$

where (a) follows from the distribution of gamma random variable H_0 (being the square of the Nakagami random variable), and (b) is calculated by applying the incomplete gamma function for integer values of m_0 to (a) and substituting $\mathcal{L}_I(s)\triangleq\mathbb{E}\left[e^{-sI}\right]$. The coverage probability for case of zero interference given in 9, i.e., $\mathbb{P}(\text{SNR}>T)$ can be trivially obtained using the above derivations and setting $I=0$. □

To complete the derivation of (8), we derive the Laplace function of interference power, I, in the following lemma.

Lemma 3. *When the serving satellite is at distance $r_0 \geq a_{\min}$ from the user, the Laplace transform of random variable I is*

$$\mathcal{L}_I(s)=\int_{a_{\min}}^{a_{\max}} f_A(a) \sum_{n_{\mathrm{I}}=1}^{\frac{N_{\mathrm{eff}}}{K}-1} \binom{\frac{N_{\mathrm{eff}}}{K}-1}{n_{\mathrm{I}}} P_{\mathrm{I}}^{n_{\mathrm{I}}}(1-P_{\mathrm{I}})^{\frac{N_{\mathrm{eff}}}{K}-1-n_{\mathrm{I}}} \cdot \left(\int_{r_0}^{r_{\max}} f_{R_n|R_0}(r_n|r_0)\mathcal{L}_{H_n}\left(sp_nG_{\mathrm{t}}(a)r_n^{-\alpha}\right) dr_n\right)^{n_{\mathrm{I}}} da, \tag{12}$$

where $f_{R_n|R_0}(r_n|r_0) = \frac{f_R(r_n)}{1-F_R(r_0)}$ is the probability density function of the distance from any visible satellite to the user conditioned on the serving distance [2, Lemma 3]. $P_{\mathrm{I}} = \frac{2r_\oplus A - r_0^2 + A^2}{4r_\oplus(r_\oplus + A) - r_0^2 + A^2}$ is obtained using [2, Lemma 4], and $\mathcal{L}_{H_n}(\cdot)$ is the Laplace transform of the random variable H_n.

Proof. Using the definition of the Laplace transform yields

$$\begin{aligned}
\mathcal{L}_I(s) &\triangleq \mathbb{E}_I\left[e^{-sI}\right] \\
&= \mathbb{E}_{A,N_{\mathrm{I}},R_n,H_n}\left[\exp\left(-s\sum_{n=1}^{N_{\mathrm{I}}} p_nG_{\mathrm{t}}(A)H_nR_n^{-\alpha}\right)\right] \\
&\overset{(a)}{=} \mathbb{E}_{A,N_{\mathrm{I}},R_n}\left[\prod_{n=1}^{N_{\mathrm{I}}}\mathbb{E}_{H_n}\left[\exp\left(-sp_nG_{\mathrm{t}}(A)H_nR_n^{-\alpha}\right)\right]\right] \\
&\overset{(b)}{=} \mathbb{E}_{A,N_{\mathrm{I}}}\left[\prod_{n=1}^{N_{\mathrm{I}}}\int_{r_0}^{r_{\max}} f_{R_n|R_0}(r_n|r_0) \cdot \mathbb{E}_{H_n}\left[\exp\left(-sp_nG_{\mathrm{t}}(A)H_nr_n^{-\alpha}\right)\right] dr_n\right] \\
&\overset{(c)}{=} \int_{a_{\min}}^{a_{\max}} f_A(a) \sum_{n_{\mathrm{I}}=1}^{\frac{N_{\mathrm{eff}}}{K}-1} \binom{\frac{N_{\mathrm{eff}}}{K}-1}{n_{\mathrm{I}}} P_{\mathrm{I}}^{n_{\mathrm{I}}}(1-P_{\mathrm{I}})^{\frac{N_{\mathrm{eff}}}{K}-1-n_{\mathrm{I}}} \cdot \left(\int_{r_0}^{r_{\max}} f_{R_n|R_0}(r_n|r_0)\mathbb{E}_{H_n}\left[\exp\left(-sp_nG_{\mathrm{t}}(a)H_nr_n^{-\alpha}\right)\right]dr_n\right)^{n_{\mathrm{I}}} da,
\end{aligned} \tag{13}$$

where (a) follows from the i.i.d. distribution of H_n and its independence from N_{I} and R_n, (b) is obtained by taking the expectation over R_n conditioned on $R_0 = r_0$, and (c) is the averaging over the binomial random variable N_{I} with the success probability P_{I}. □

Another metric that enlightens the worldwide coverage provided by a LEO constellation, regardless of the users' locations, i.e., their latitudes, is global coverage probability, denoted by $P_{\mathrm{c}}^{\mathrm{Global}}$. The metric is defined as the weighted summation of coverage probability over all the potential global users' latitudes as follows.

Lemma 4. *The global coverage probability, irrespective of the ground user's latitude, is given as $P_{\mathrm{c}}^{\mathrm{Global}} = \int_{-\pi/2}^{\pi/2} P_{\mathrm{c}}(\phi_{\mathrm{u}})\, f_{\phi_{\mathrm{u}}}(\phi_{\mathrm{u}}) d\phi_{\mathrm{u}}$, where $f_{\phi_{\mathrm{u}}}(\phi_{\mathrm{u}})$ is the PDF of the population distribution over different latitudes.*

IV. Numerical Results

We verify our analytical findings on the coverage probability of a multi-altitude constellation through Monte Carlo simulations with four commercial constellations. Moreover, we show the effect of altitude, the constellation size, and user's latitude on the coverage probability. According to the detailed specifications given in Table I, the satellites of each constellation are distributed on multiple orbital shells, each of which has the same number of satellites while their altitudes and inclination angles are different. To plot the analytical coverage probability for each constellation, the altitude is assumed to be uniformly distributed ranging from the minimum altitude to the maximum altitude of the given constellation.

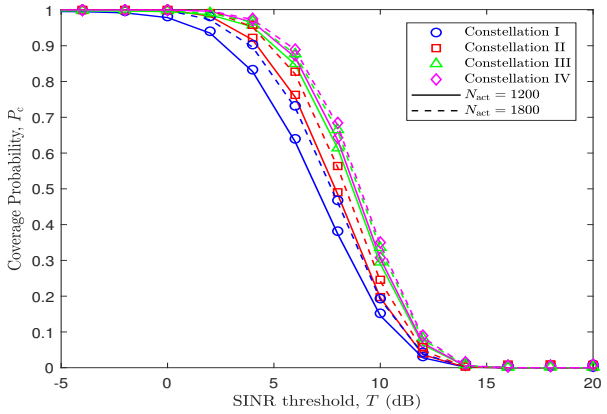

Fig. 2. Verification of Proposition 2 with simulations for the four constellations given in Table I. The user is located at $\phi_{\mathrm{u}} = 25°$.

A well-known sectorized antenna pattern similar to [6]–[8] is adopted to approximate the alignment of main lobes on the desired link and alignment of side lobes on interfering links[1]. The maximum antenna gains given in Table I are chosen to satisfy the received average SNR of 10 dB for each constellation, i.e., higher gains are chosen for constellations with higher altitude range to compensate for more severe path loss. The maximum gain of user's antenna is set to 31.8 dBi as given in [9]. Similar to [6], the misalignment between interfering satellites' and user's antenna beams is considered by assuming 13 dB lower antenna gain for them.

To compensate for the uneven satellite distribution along latitudes, N_{eff} is calculated for each orbital shell in Table I per Proposition 1. The summation of the obtained N_{eff} for all orbital shells returns the overall N_{eff} for a given constellation. The minimum elevation angle and the path-loss exponent are set to $\theta_{\min} = 20°$ and $\alpha = 2$, respectively. A practical fading distribution, i.e., Rician fading with parameter 6.5 is assumed for simulations to equivalently represent the Nakagami fading used for analysis. The transmitted power is set to $p_{\mathrm{t}} = 10$ W. The operating frequency, total bandwidth, the number of frequency channels, and the noise power per channel are assumed to be 20 GHz, 2 GHz, $K = 50$, and $\sigma^2 = -95$ dBm, respectively. In all the figures, *the lines and the markers represent the analytical results and simulations, respectively.*

[1]In two special cases the reception of interference may happen through the main beams of satellites or user to/from a side lobe. The first case occurs when a user is within the overlapping coverage area of several satellites so that it receives interference through their main beams. The second scenario may happen if some interfering satellites and the server are in close proximity or have almost similar true anomaly so that the satellites' side lobes interfere with the user's main lobe. Such scenarios can be avoided by implementing frequency reuse so that the server and its neighboring satellites are allocated to different channels.

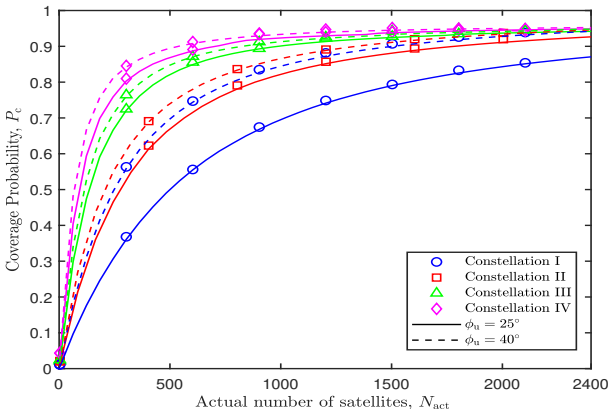

Fig. 3. The effect of constellation size on coverage probability of the constellations, given in Table I, for $\phi_{\text{u}} \in \{25°, 40°\}$ and $T = 5$ dB.

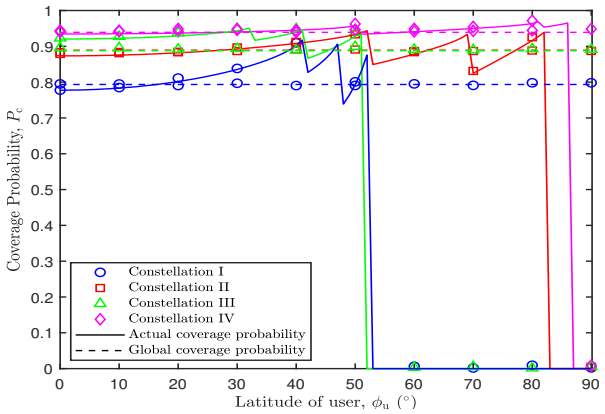

Fig. 4. The effect of user's latitude on the coverage probability for constellations given in Table I with $T = 5$ and $N_{\text{act}} = 1800$.

Figure 2 validates the expression in Proposition 2 for the constellations given in Table I with $N_{\text{act}} = 1200$ and 1800. The variation in the coverage probability is affected by the visibility probability and the path-loss attenuation. For lower thresholds, the performance is upper bounded by the probability of being visited by at least one satellite. According to the figure, for all constellations, there is at least one visible satellite that serves the user. By increasing the SINR threshold, Constellations III and IV outperform other constellations due to their higher altitude range and, consequently, higher probability of being visible to the users. In other words, for constellations III and IV, the user may connect to a satellite with a relatively higher elevation angle which compensates for the higher path loss attenuation of those constellations.

In Fig. 3, the coverage probability of the four constellations is depicted versus the total number of satellites for $\phi_{\text{u}} = 25°$ and $40°$. Higher altitude range for Constellations III and IV results in a better visibility probability and, consequently, better coverage probability at the given latitudes. The probability of coverage converges to a fixed value, when the constellation size exceeds a certain limit, implying that increasing the constellation size does not necessarily improve performance.

The effect of the user's latitude on the coverage probability is shown in Fig. 4. The varying behaviour of the plots is justifiable due to changes in the number of visible satellites with the user's latitude. The asymmetric local maxima at the inclination angles of each orbital shell is due to the reduction in the interfering satellites as well as the increase in the satellite density and, consequently, a rise in the probability of connecting to a nearer satellite. The peak points are followed by sharp local minima caused by loss of connection with the best available server. The coverage drops more significantly at larger inclination angles as the number of visible satellites to the user decreases drastically. The performance is more uniform for Constellation IV since the variation in the visibility of satellites is less significant due to its higher altitude.

The global coverage probability for all constellations is also depicted in Fig. 4 using Lemma 4. The population distribution over latitudes is obtained from NASA's socioeconomic data and applications center [10]. As can be seen, Constellation IV provides superior global coverage as those middle- and high-latitude regions are totally covered by its inclined orbits.

V. Conclusions

Stochastic geometry-based modeling and analysis of a multi-altitude LEO network is proposed, assuming satellites are distributed on several orbital shells with different altitudes and inclination angles. As illustrated through the numerical results, deploying satellites on several orbital shells with different inclination angles to cover all the latitudes, results in a more promising global coverage probability. Although, given a fixed number of satellites and nearly the same altitude range, the performance is inferior for lower latitudes as the density, and consequently, the visibility probability is lower compared to constellations with lower inclination angles.

References

[1] X. Lu, M. Salehi, M. Haenggi, E. Hossain, and H. Jiang, "Stochastic geometry analysis of spatial-temporal performance in wireless networks: A tutorial," *IEEE Communications Surveys and Tutorials*, vol. 23, no. 4, pp. 2753–2801, Aug. 2021.

[2] N. Okati, T. Riihonen, D. Korpi, I. Angervuori, and R. Wichman, "Downlink coverage and rate analysis of low Earth orbit satellite constellations using stochastic geometry," *IEEE Transactions on Communications*, vol. 68, no. 8, pp. 5120–5134, Aug. 2020.

[3] N. Okati and T. Riihonen, "Stochastic analysis of satellite broadband by mega-constellations with inclined LEOs," in *Proc. IEEE 31st Annual International Symposium on Personal, Indoor and Mobile Radio Communications*, Sep. 2020.

[4] ——, "Nonhomogeneous stochastic geometry analysis of massive LEO communication constellations," *IEEE Transactions on Communications*, vol. 70, no. 3, pp. 1848–1860, Jan. 2022.

[5] A. Talgat, M. A. Kishk, and M.-S. Alouini, "Stochastic geometry-based analysis of LEO satellite communication systems," *IEEE Communications Letters*, vol. 25, no. 8, pp. 2458–2462, Aug. 2021.

[6] A. G. Bole, A. Wall, and A. Norris, *Radar and ARPA Manual: Radar, AIS and Target Tracking for Marine Radar Users, chapter 2*. Butterworth-Heinemann, 2013.

[7] M. Di Renzo, "Stochastic geometry modeling and analysis of multi-tier millimeter wave cellular networks," *IEEE Transactions on Wireless Communications*, vol. 14, no. 9, pp. 5038–5057, May 2015.

[8] S. Singh, M. N. Kulkarni, A. Ghosh, and J. G. Andrews, "Tractable model for rate in self-backhauled millimeter wave cellular networks," *IEEE Journal on Selected Areas in Communications*, vol. 33, no. 10, pp. 2196–2211, May 2015.

[9] I. del Portillo, B. G. Cameron, and E. F. Crawley, "A technical comparison of three low Earth orbit satellite constellation systems to provide global broadband," *Acta Astronautica*, vol. 159, pp. 123–135, 2019.

[10] "Gridded population of the world: Administrative unit center points with population estimates," *Center for International Earth Science Information Network Columbia University, NASA Socioeconomic Data and Applications Center*, 2018, available: https://doi.org/10.7927/H4BC3WMT.